ELSEVIER

Engineering Structures 24 (2002) 59–72

ENGINEERING STRUCTURES

www.elsevier.com/locate/engstruct

Comparisons of concrete-encased composite column strength provisions of ACI code and AISC specification

C.C. Weng *, S.I. Yen

Department of Civil Engineering, National Chiao Tung University, Hsinchu, 30050, Taiwan, ROC

Received 20 September 2000; received in revised form 9 May 2001; accepted 26 June 2001

Abstract

In the ACI-318 code (1999) and AISC-LRFD specification (1993), different approaches are used for the design of concrete-encased composite columns. The calculated member strengths based on these two design provisions may show significant difference in some cases. The objective of this study is to investigate the difference between these two approaches and to evaluate the accuracy of their strength predictions by comparing to 78 physical test results done by previous researchers. This comparative study indicates that the ACI-318 approach generally gives closer predictions than the AISC-LRFD does. The statistical results show that the ACI-to-experimental capacity ratio has a mean value of 0.90 with a coefficient of variation (COV) of 15% and the AISC-to-experimental capacity ratio has a mean value of 0.73 with a COV of 21%. Also investigated herein are the difference of design philosophy between the design provisions, the failure mode of the tested specimens, the column strength interaction diagram, and the effect of steel ratio on the accuracy of the strength predictions. © 2001 Elsevier Science Ltd. All rights reserved.

Keywords: Concrete-encased composite column; Physical test result; Design provision; Statistical result; Design philosophy; Failure mode; Steel ratio

1. Introduction

The composite concrete and steel structural system combines the rigidity and formability of reinforced concrete with the strength of structural steel to produce an economic structure. For concrete-encased composite structural members, an additional advantage is that the concrete used for encasing a structural steel not only increases its stiffness, but also protects it from fire damage and local buckling failure.

In the United States, specific regulations for the design of concrete-encased composite columns are included in two different sets of structural design specifications. One is the building code for structural concrete of the American Concrete Institute (ACI)[1], and the other is the specification of Load and Resistance Factor Design (LRFD) published by American Institute of Steel Construction (AISC) [2]. The ACI-318 provisions (1999) for the design of the encased composite columns follow the same procedure as that for the reinforced concrete columns. In contrast, the AISC-LRFD provisions (1993) are based on analogous to the steel column design. Both ACI and AISC design provisions are applied to concrete-encased structural steel columns and to concrete-filled pipes or tubing.

The AISC-LRFD rules specifically require at least 4% steel ratio of the composite section comprised of structural steel. However, the ACI rules have no such limitation on steel ratio. In addition, the former is recommended for symmetric composite section, but the latter is recommended for both symmetric and unsymmetrical sections [3,4]. It is noted that the above-mentioned specifications often give significantly different values of calculated ultimate member strengths [5,6].

The objective of this study is to investigate the differences between the ACI and the AISC approaches for the design of concrete-encased composite columns and to evaluate how well they model the actual column behavior through a series of statistical comparisons. The studies are made to compare the predicted strengths by using the ACI and the AISC approaches with 78 physical test results of encased composite column done by previous researchers such as Mirza, Ricles, Yamada, Naka, Wakabayashi, Yokoo and Stevens [7–13].

* Corresponding author. Tel.: +886-3-5726507; fax: +886-3-726507.

E-mail address: weng@cc.nctu.edu.tw (C.C. Weng).

0141-0296/02/$ - see front matter © 2001 Elsevier Science Ltd. All rights reserved.
PII: S0141-0296(01)00067-0

Nomenclature

A_c, A_r area of concrete and longitudinal reinforcement, respectively
A_s, A_w area of steel shape and web of steel shape, respectively
B_1 moment magnifier suggested in AISC-LRFD specification
c_1, c_2, c_3 numerical coefficients, c_1=0.7, c_2=0.6 and c_3=0.2 for encased composite columns
c_r thickness of concrete cover from center of longitudinal reinforcement to the edge of section in the plane of bending
D overall dimension in the direction of buckling
E_c elastic modulus of concrete
E_m modified modulus of elasticity
F_{cr} critical stress of column
F_{my} modified yield stress
F_y specified yield strength of steel shape
F_{yr} specified yield strength of longitudinal reinforcement
f_c' specified compressive strength of concrete
h_1 width of composite cross section perpendicular to the plane of bending
h_2 width of composite cross section parallel to the plane of bending
I_g gross section moment of inertia
KL effective length
M_n nominal moment capacity without axial load
M_u factored moment
M_{u1}, M_{u2} the smaller and the larger required moments applied at both ends of the column, respectively
P_0 composite column capacity under uniaxial compression
P_c critical load of column
P_n nominal axial compressive capacity
P_u factored axial load
r radius of gyration
r_m modified radius of gyration
Z plastic section modulus of steel shape
δ moment magnifier suggested in ACI-318 code
ϕ_b resistance factor for bending, taken as 0.9
ϕ_c resistance factor for compression, taken as 0.85
λ_c slenderness parameter

2. Review of design methods

2.1. ACI-318 approach

In the US, the ACI building code has been the sole major reference for the design of composite columns until the publication of the AISC-LRFD specification in 1986. The following sections briefly introduce the concerned strength provisions for the concrete-encased composite columns as recommended in section 10.16 of the ACI-318 building code (1999).

2.1.1. Axial compressive strength

Under uniaxial compression, the nominal compressive strength, P_n, of a concrete-encased composite column can be found by summing up the axial-load capacities of the materials that make up the cross section. This leads to

$$P_n = 0.8P_0 \tag{1a}$$

$$P_0 = 0.85f_c'A_c + F_{yr}A_r + F_yA_s \tag{1b}$$

where

P_0 column capacity under uniaxial compression
f_c' compressive strength of concrete
A_c area of concrete
F_{yr} yield strength of longitudinal reinforcement
A_r area of longitudinal reinforcement
F_y yield strength of steel shape
A_s area of steel shape

The nominal axial compressive strength P_n for an encased composite column is limited to $0.8P_0$ owing to a minimum eccentricity under axial load for all designed columns.

2.1.2. Second-order effect

The ACI-318 approach requires that all columns be designed as beam-columns transferring both shear and bending moment at joints. The columns shall be designed according to the factored forces and moments from a second-order analysis. As an alternative to the second-order analysis, design can be based on first-order elastic analysis and moment magnification approach. The moment magnifier δ is expressed as

$$\delta=\frac{0.6+0.4\frac{M_{u1}}{M_{u2}}}{1-\frac{P_u}{0.75P_c}}\geq 1 \tag{2a}$$

with M_{u1}, M_{u2}=the smaller and the larger required moments at the ends of the column, respectively; P_u=factored axial load; and P_c=critical load of column, taken as

$$P_c=\frac{\pi^2 EI}{(KL)^2} \tag{2b}$$

where KL=effective length; EI=flexural rigidity.

To account for the variations in stiffness due to cracking, creep and nonlinearity of concrete, the EI value of above equation can be conservatively taken as $0.25E_cI_g$, in which E_c is the concrete elastic modulus and I_g is the gross section moment of inertia. It is also noted that the second-order effect can be neglected if the column slenderness ratio, KL/r, meets the following requirement:

$$\frac{KL}{r}\leq 34-12\left(\frac{M_{u1}}{M_{u2}}\right) \tag{3}$$

2.1.3. Flexural and axial loads

The ACI-318 provisions for the strength interaction between axial and flexural loads for concrete-encased composite columns are essentially the same as those for ordinary reinforced concrete columns. They are based on a strain compatibility analysis at the limit state to develop a thrust–moment (P–M) interaction relation. The following assumptions are made in the analysis:

- Plane section remains plane.
- The maximum concrete compressive strain is limited to 0.003.
- The Whitney stress block, having a magnitude of $0.85f_c'$, is used for the concrete.
- Tensile strength of the concrete is neglected.
- Strain hardening of steel shape and rebar is neglected.

2.2. AISC-LRFD approach

Although the AISC specification has included design provisions for composite beams with shear connectors since 1961, the design requirements for composite columns were not recommended until the publication of the first edition of the AISC-LRFD specification in 1986. The concept of extending the steel column design methodology to the composite columns using the modified properties was first introduced by Furlong [14]. Modified yield stress F_{my}, modulus of elasticity E_m and radius of gyration r_m were incorporated into steel column design equations for the design of composite columns. This procedure was presented by the Task Group 20 of the Structural Stability Research Council (SSRC) in 1979 [15]. The following sections briefly introduce the concerned strength provisions for encased composite columns as recommended in Chapter I of the AISC-LRFD specification (1993).

2.2.1. Axial compressive strength

The capacity of an encased column is determined from the same equations as that for bare steel columns except the formulas being entered with modified properties F_{my}, E_m and r_m. The nominal axial compressive strength of an encased composite column is

$$P_n=A_sF_{cr} \tag{4}$$

where A_s is the area of the steel shape and F_{cr} is the critical stress of the column given by the following equations:

$$F_{cr}=(0.658^{\lambda_c^2})F_{my} \text{ for } \lambda_c\leq 1.5 \tag{5}$$

and

$$F_{cr}=\left(\frac{0.877}{\lambda_c^2}\right)F_{my} \text{ for } \lambda_c>1.5 \tag{6}$$

where $\lambda_c=(KL/\pi r_m)\sqrt{F_{my}/E_m}$; F_{my}=modified yield stress; r_m=modified radius of gyration; E_m=modified modulus of elasticity.

The modified properties F_{my}, E_m and r_m account for the contribution of concrete and rebars in the composite section. The modified values F_{my} and E_m can be determined by the following equations:

$$F_{my}=F_y+c_1F_{yr}\frac{A_r}{A_s}+c_2f_c'\frac{A_c}{A_s} \tag{7}$$

and

$$E_m=E_s+c_3E_c\frac{A_c}{A_s} \tag{8}$$

where c_1, c_2, c_3=numerical coefficients, for encased composite columns c_1=0.7, c_2=0.6 and c_3=0.2.

2.2.2. Second-order effect

For columns designed on the basis of elastic analysis, the factored moment M_u shall be determined by a second-order analysis or by the moment magnification method. The moment magnifier B_1 is expressed as

$$B_1=\frac{0.6+0.4\frac{M_{u1}}{M_{u2}}}{1-\frac{P_u\lambda c^2}{A_sF_{my}}}\geq 1 \quad (9)$$

2.2.3. Flexural and axial loads

For an encased composite column symmetrical about the plane of bending, the interaction of compressive and flexural loads should be limited by the following bilinear relationship:

$$\frac{P_u}{\phi_c P_n}+\frac{8M_u}{9\phi_b M_n}\leq 1.0 \quad \text{for } P_u\geq 0.2\phi_c P_n \quad (10)$$

and

$$\frac{P_u}{2\phi_c P_n}+\frac{M_u}{\phi_b M_n}\leq 1.0 \quad \text{for } P_u< 0.2\phi_c P_n \quad (11)$$

where

P_u	factored axial load
M_u	factored moment
P_n	nominal axial compressive capacity
M_n	nominal flexural capacity without axial force
ϕ_c	0.85
ϕ_b	0.9

To determine the nominal flexural capacity M_n, the commentary of AISC-LRFD specification provides an approximate equation for doubly symmetric composite sections as follows:

$$M_n=ZF_y+\frac{1}{3}(h_2-2c_r)A_rF_{yr}+\left(\frac{h_2}{2}-\frac{A_wF_y}{1.7f_c'h_1}\right)A_wF_y \quad (12)$$

where

Z	plastic section modulus of steel shape
h_1	width of composite cross section perpendicular to the plane of bending
h_2	width of composite cross section parallel to the plane of bending
c_r	thickness of concrete cover from center of longitudinal reinforcement to the edge of section in the plane of bending
A_w	web area of steel shape

3. Survey of previous tested composite columns

In 1996, Mirza et al. studied sixteen encased composite columns subjected to strong axis bending in which second-order effects were significant. The height of the columns was 4 meters for all specimens. As observed from the tests, concrete strain in extreme compression fiber reached around 0.0025–0.004 prior to failure of specimens. It was noted that the bonding at the interface of steel flange and the surrounding concrete had little effect on the ultimate capacity of the composite column [7].

Ricles et al. (1994) presented experimental results of eight concrete-encased composite columns. The cross-sectional dimensions of the columns were 406×406 mm, which were relatively large in scale as compared to the specimens of other researchers. All columns were subjected to strong axis bending and were tested under monotonic axial load and cyclic lateral load. It was observed that the maximum capacity of the specimens developed after the yielding of longitudinal reinforcements and steel flange. The test results also indicated that the shear studs were not effective in enhancing the flexural strength [8].

Experimental results of five small-scale encased composite columns presented by Yamada et al. (1991) are collected in this study. All specimens were subjected to strong axis bending and the applied loading included combinations of axial and transverse forces at both ends of the column. Test results showed that most of the specimens reached the maximum capacity when concrete spalled and rebars yielded in the tension side [9].

Naka et al. (1977) presented experimental results of four pinned-ended encased composite columns subjected to strong axis bending. The applied loading included combinations of axial and bending forces. Naka et al. indicated that the failure mode of specimens could be divided into two categories: (1) concrete crushing failure and local buckling of steel flange in compressive side; and (2) concrete crushing failure and buckling of rebars in compression side and yielding of rebars in tension side [10].

In 1971, Wakabayashi et al. carried out test results of four pinned-ended encased composite columns. All specimens were subjected to strong axis bending and the applied loading included static axial load and transverse force. It was observed that as the load was increased to the ultimate capacity of the columns, buckling of longitudinal reinforcements in compression side and yielding of rebars in tension side were found for most of the tested specimens [11].

Yokoo et al. (1967) presented experimental results of nineteen simply supported encased composite short columns. It was reported that as the load approached to the failure condition, wide cracks appeared on the bottom face for all specimens, and failure took place due to crushing of the concrete [12].

In 1965, Stevens presented experimental results of 22 pinned-ended encased composite columns subjected to weak axis bending. The applied loading included static

Table 1
Composite column test data carried out by Mirza et al. (1996)

Specimen no.	$B\times D$ (mm)	Steel shape $d\times b_f\times t_w\times t_f$ (mm)	A_r (mm^2)	F_{ys} (MPa)	F_{yr} (MPa)	f_c' (MPa)	KL (mm)	M_{TEST} (kN-m)	P_{TEST} (kN)
1	240×240	96×100×5.1×8.6	284	293.4	565.0	27.0	4000	64.1	950.0
2	240×240	96×100×5.1×8.6	284	293.4	565.0	27.0	4000	63.2	550.0
3	240×240	96×100×5.1×8.6	284	293.4	565.0	27.6	4000	78.2	570.0
4	240×240	96×100×5.1×8.6	284	311.2	634.0	25.5	4000	79.8	307.5
5	240×240	96×100×5.1×8.6	284	293.4	565.0	24.8	4000	66.0	154.3
6	240×240	96×100×5.1×8.6	284	293.4	565.0	28.5	4000	65.6	95.0
7	240×240	96×100×5.1×8.6	284	311.2	634.0	27.4	4000	82.2	925.0
8	240×240	96×100×5.1×8.6	284	311.2	634.0	27.4	4000	76.0	775.0
9	240×240	96×100×5.1×8.6	284	293.4	565.0	26.5	4000	82.3	540.0
10	240×240	96×100×5.1×8.6	284	293.4	565.0	27.0	4000	93.8	352.5
11	240×240	96×100×5.1×8.6	284	293.4	565.0	27.2	4000	73.5	107.5
12	240×240	96×100×5.1×8.6	284	311.2	634.0	27.4	4000	72.0	927.0
13	240×240	96×100×5.1×8.6	284	311.2	634.0	27.4	4000	69.9	720.0
14[a]	240×240	96×100×5.1×8.6	284	311.2	634.0	25.5	4000	83.0	540.0
15[a]	240×240	96×100×5.1×8.6	284	311.2	634.0	25.5	4000	79.9	296.0
16[a]	240×240	96×100×5.1×8.6	284	311.2	634.0	25.5	4000	68.7	100.0

[a] *: Test results of these specimens are plotted in Fig. 3 to compare with the P-M curves constructed based on ACI code and AISC-LRFD specification.

axial forces at both ends of the specimen with various eccentricities. Two failure modes were observed from the tests. They were (1) crushing of concrete on one face near the top of structural steel shape, and (2) crushing of concrete on one face and yielding of steel in compression, being accompanied by tensile cracks of concrete on the opposite face [13].

4. Comparisons between test results and predicted capacities

Listed in Tables 1–7 are the dimensions, material properties and the test results of 78 encased composite columns collected in this study. In Tables 8–14, test results are compared with the predicted capacities using ACI-318 and AISC-LRFD approaches. In these tables, P_{TEST} represents the ultimate column capacity obtained from the test results done by previous researchers; P_{ACI} and P_{LRFD} are the predicted nominal capacities using ACI-318 and AISC-LRFD approaches, respectively. All predicted values are carried out according to the given provisions except that the strength reduction factors are taken as 1.0. Also given in the tables are the ACI-to-experimental capacity ratio and the AISC-to-experimental capacity ratio. More detailed comparisons are presented as follows.

4.1. Comparisons

Table 8 shows the comparisons between the test results done by Mirza et al. (1996) and the predicted capacities using ACI-318 and AISC-LRFD approaches. This table reveals that all the predicted capacities based on the ACI-318 approach are conservative (up to 28%) as compared with the test results (except specimen No.

Table 2
Composite column test data carried out by Ricles et al. (1994)

Specimen no.	$B\times D$ (mm)	Steel shape	A_r (mm^2)	F_{ys} (MPa)	F_{yr} (MPa)	f_c' (MPa)	KL (mm)	M_{TEST} (kN-m)	P_{TEST} (kN)
1	406×406	W8×40	3148	373.7	455.8	32.7	2489	626.0	1490
2	406×406	W8×40	1548	373.7	434.4	34.5	2489	593.0	1490
3[a]	406×406	W8×40	4645	373.7	434.4	30.9	1930	784.0	1490
4	406×406	W8×40	2581	373.7	448.2	31.1	1930	670.0	1490
5[a]	406×406	W8×40	4645	373.7	434.4	34.5	1930	776.0	1490
6	406×406	W8×40	2581	373.7	448.2	35.8	1930	667.0	1490
7	406×406	W8×40	4645	373.7	434.4	62.9	1930	840.0	1490
8	406×406	W8×40	4645	373.7	434.4	64.5	1930	832.0	1490

[a] Test results of these specimens are plotted in Fig. 4 to compare with the P-M curves constructed based on ACI code and AISC-LRFD specification.

Table 3
Composite column test data carried out by Yamada et al. (1991)

Specimen no.	$B\times D$ (mm)	Steel shape $d\times b_f\times t_w\times t_f$ (mm)	A_r (mm^2)	F_{ys} (MPa)	F_{yr} (MPa)	f_c' (MPa)	KL (mm)	M_{TEST} (kN-m)	P_{TEST} (kN)
1[a]	125×125	80×60×2.0×2.0	142	270.3	381.3	33.2	625	17.9	121.0
2[a]	125×125	80×60×2.0×2.0	142	270.3	381.3	28.5	625	17.9	217.0
3	125×125	80×60×2.0×2.0	142	270.3	381.3	31.8	625	17.5	483.0
4	125×125	80×40×2.0×2.0	142	270.3	381.3	26.6	625	15.6	200.0
5	125×125	50×60×3.2×3.2	142	290.3	381.3	33.4	625	17.2	223.0

[a] Test results of these specimens are plotted in Fig. 5 to compare with the P-M curves constructed based on ACI code and AISC-LRFD specification.

Table 4
Composite column test data carried out by Naka et al. (1977)

Specimen no.	$B\times D$ (mm)	Steel shape $d\times b_f\times t_w\times t_f$ (mm)	A_r (mm^2)	F_{ys} (MPa)	F_{yr} (MPa)	f_c' (MPa)	KL (mm)	M_{TEST} (kN-m)	P_{TEST} (kN)
1[a]	240×300	180×120×4.5×12.0	2323	344.8	461.3	25.5	1030	197.4	1470.0
2[a]	240×300	180×120×4.5×12.0	2323	344.8	461.3	25.5	1030	235.0	980.0
3[a]	240×300	180×120×4.5×12.0	2323	344.8	461.3	25.5	1030	228.4	490.0
4[a]	240×300	180×120×4.5×12.0	2323	344.8	461.3	25.5	1030	214.0	0.0

[a] Test results of these specimens are plotted in Fig. 6 to compare with the P-M curves constructed based on ACI code and AISC-LRFD specification.

Table 5
Composite column test data carried out by Wakabayashi et al. [11]

Specimen no.	$B\times D$ (mm)	Steel shape $d\times b_f t_w\times t_f$ (mm)	A_r (mm^2)	F_{ys} (MPa)	F_{yr} (MPa)	f_c' (MPa)	KL (mm)	M_{TEST} (kN-m)	P_{TEST} (kN)
1	210×210	150×100×6.0×9.0	284	299.9	360.6	21.1	850	67.7	0.0
2	210×210	150×100×6.0×9.0	284	306.1	360.6	26.4	850	72.4	293.6
3	210×210	150×100×6.0×9.0	284	306.1	360.6	28.9	850	67.7	587.1
4	210×210	150×100×6.0×9.0	284	306.1	360.6	27.0	850	59.0	880.7

2). The predicted capacities based on the AISC-LRFD approach are found even more conservative (up to 42%).

Table 9 displays the comparisons between the test results done by Ricles et al. (1994) and the predicted capacities using ACI-318 and AISC-LRFD approaches. The predicted capacities using these two approaches are conservative (up to 22 and 40%, respectively) as compared with the test results.

Comparisons between the test results done by Yamada et al. (1991) and the predicted capacities using ACI-318 and AISC-LRFD approaches are shown in Table 10. It is observed that the predicted capacities based on the ACI-318 approach are conservative up to 44% and those based on the AISC-LRFD approach are conservative up to 69%.

Table 11 lists the comparative results of the predicted capacities using ACI-318 and AISC-LRFD approaches to the test results done by Naka et al. (1977). The table shows that the predicted capacities (except specimen No. 3) based on the ACI-318 approach are reasonably conservative (up to 5%) as compared with the test results and those based on the AISC-LRFD approach are much more conservative (up to 31%).

The predicted results obtained from using ACI-318 and AISC-LRFD approaches compared with test results done by Wakabayashi et al. (1971) are presented in Table 12. It is found that the predicted capacities based on the ACI-318 approach somewhat overestimate the test strengths (up to 12%), with the exception of specimen No. 1. On the contrary, those based on the AISC-LRFD approach are conservative (up to 24%), except specimen No. 1.

Table 13 displays the comparisons between the test results done by Yokoo et al. (1967) and the predicted capacities using ACI-318 and AISC-LRFD approaches. It is seen that the predicted capacities for some specimens based on the ACI-318 and the AISC-LRFD approaches are slightly unconservative (up to 21 and 5%

Table 6
Composite column test data carried out by Yokoo et al. [12]

Specimen no.	$B\times D$ (mm)	Steel shape $d\times b_f\times t_w\times t_f$ (mm)	A_r (mm^2)	F_{ys} (MPa)	F_{yr} (MPa)	f_c' (MPa)	KL (mm)	M_{TEST} (kN-m)	P_{TEST} (kN)
1	210×210	154×100×7.7×10.5	–	260.0	–	17.6	630	37.5	892.7
2	210×210	152×101×8.1×10.3	–	250.2	–	16.5	630	35.4	843.7
3	210×210	153×101×7.6×10.4	–	260.0	–	17.4	630	33.0	784.8
4	210×210	153×101×7.6×10.5	–	275.7	–	11.5	630	29.8	709.3
5	210×210	153×100×9.2×10.5	–	351.2	–	15.3	630	52.2	497.4
6	210×210	152×100×7.9×10.5	–	271.7	–	17.6	630	57.7	578.8
7	210×210	153×101×8.7×10.4	–	351.2	–	11.8	630	57.7	549.4
8	210×210	152×100×7.9×10.3	–	250.2	–	15.4	630	50.5	480.7
9	210×210	152×101×7.6×10.2	–	271.7	–	17.7	630	64.3	306.1
10	210×210	153×101×8.6×10.2	–	351.2	–	19.8	630	78.3	372.8
11	210×210	152×102×7.6×10.0	–	271.7	–	18.0	630	58.7	279.6
12	210×210	153×102×8.9×10.1	–	351.2	–	11.8	630	70.5	335.0
13	210×210	152×102×7.9×10.2	–	274.7	–	14.4	630	65.9	157.0
14	210×210	152×101×8.0×10.2	–	274.7	–	18.1	630	70.1	166.8
15	210×210	152×101×8.0×10.2	–	274.7	–	18.2	630	67.2	159.9
16	210×210	152×101×7.8×10.5	–	274.7	–	11.9	630	61.6	146.7
17[a]	210×210	153×101×7.6×10.5	–	275.7		17.4	630	22.3	531.7
18[a]	210×210	152×101×7.8×10.4	–	250.2		14.9	630	27.3	260.0
19[a]	210×210	152×101×7.8×10.4	–	274.7	–	15.8	630	28.9	68.7

[a] Specimen nos 17 to 19 were bent about minor axis.

Table 7
Composite column test data carried out by Stevens [13]

Specimen no.	$B\times D$ (mm)	Steel stanchion	A_r (mm^2)	F_{ys} (MPa)	F_{yr} (MPa)	f_c' (MPa)	KL (mm)	M_{TEST} (kN-m)	P_{TEST} (kN)
1	165×178	5.0×4.5 (20 lb)	–	231.7	–	19.3	2083	13.7	716.1
2	165×178	5.0×4.5 (20 lb)	–	231.7	–	19.3	2083	14.3	747.3
3	165×178	5.0×4.5 (20 lb)	–	231.7	–	19.3	2083	17.2	898.5
4	165×178	5.0×4.5 (20 lb)	–	231.7	–	19.3	2083	20.6	1014.1
5	165×178	5.0×4.5 (20 lb)	–	231.7	–	19.3	726	18.8	738.4
6	165×178	5.0×4.5 (20 lb)	–	231.7	–	19.3	1156	12.7	996.4
7	165×178	5.0×4.5 (20 lb)	–	231.7	–	19.3	1156	18.5	729.5
8	165×178	5.0×4.5 (20 lb)	–	231.7	–	19.3	2083	15.9	627.2
9	165×178	5.0×4.5 (20 lb)	–	231.7	–	19.3	2997	9.1	716.1
10	165×178	5.0×4.5 (20 lb)	–	231.7	–	19.3	2997	13.4	529.3
11	165×178	5.0×4.5 (20 lb)	–	231.7	–	19.3	3886	11.2	440.4
12	165×178	5.0×4.5 (20 lb)	–	231.7	–	19.3	3886	13.2	346.9
13	165×178	5.0×4.5 (20 lb)	–	231.7	–	19.3	3886	16.7	329.2
14	305×406	12.0×8.0 (65 lb)	–	222.7	–	17.4	3048	75.9	2989.1
15	305×406	12.0×8.0 (65 lb)	–	222.7	–	16.3	3048	109.8	2161.7
16	305×406	12.0×8.0 (65 lb)	–	222.7	–	27.0	3048	116.4	2290.7
17	305×406	12.0×8.0 (65 lb)	–	222.7	–	18.5	3048	122.4	1605.7
18	305×406	12.0×8.0 (65 lb)	–	222.7	–	18.5	3048	133.8	1316.6
19	305×406	12.0×8.0 (65 lb)	–	222.7	–	19.3	3048	148.0	1165.4
20	305×406	12.0×8.0 (65 lb)	–	222.7	–	18.8	3048	156.6	1027.5
21	305×406	12.0×8.0 (65 lb)	–	222.7	–	21.2	3048	157.4	885.2
22	305×406	12.0×8.0 (65 lb)	–	222.7	–	20.7	3048	151.9	747.3

respectively) to the test strengths. But the predicted capacities for other specimens are conservative (up to 13 and 43% for ACI-318 and AISC-LRFD, respectively).

As shown in Table 14, the predicted capacities using ACI-318 and AISC-LRFD approaches are compared with test results done by Stevens (1965). This table shows that the predicted capacities based on the ACI-318 approach are somewhat unconservative (up to 9%) to the test results for four specimens but are conservative (up to 29%) for the others. For those based on the AISC-LRFD approach, all predictions are found to be quite conservative (up to 50%).

Table 8
Comparison between test results (Mirza et al. [7]) and predicted values using ACI code and AISC-LRFD specification

Specimen no.	Eccentricity (mm)	P_{TEST} (kN)	P_{ACI} (kN)	P_{LRFD} (kN)	P_{ACI}/P_{TEST}	P_{LRFD}/P_{TEST}
1	39.7	950.0	785.5	616.9	0.827	0.649
2	65.8	550.0	599.1	468.8	1.089	0.852
3	105.6	570.0	445.7	344.3	0.782	0.604
4	200.3	307.5	253.1	215.3	0.823	0.700
5	370.7	154.3	134.3	115.7	0.871	0.750
6	632.4	95.0	81.8	69.8	0.862	0.735
7	48.9	925.0	733.0	585.8	0.792	0.633
8	57.6	775.0	672.5	536.9	0.868	0.693
9	106.0	540.0	450.1	350.1	0.834	0.648
10	209.4	352.5	254.4	205.1	0.722	0.582
11	628.5	107.5	85.8	72.5	0.799	0.674
12	41.7	927.0	792.6	634.3	0.855	0.684
13	59.1	720.0	662.8	528.9	0.920	0.735
14	98.4	540.0	463.9	379.9	0.859	0.703
15	206.3	296.0	257.1	216.2	0.869	0.730
16	621.8	100.0	87.6	76.5	0.876	0.765
				Mean value:	0.853	0.696
				Standard deviation	0.079	0.067
				Coefficient of variation	9.2%	9.6%

Table 9
Comparison between test results (Ricles and Paboojian [8]) and predicted values using ACI code and AISC-LRFD specification

Specimen no.	Eccentricity (mm)	P_{TEST} (kN)	P_{ACI} (kN)	P_{LRFD} (kN)	P_{ACI}/P_{TEST}	P_{LRFD}/P_{TEST}
1	419.0	1490.0	1371.8	1038.2	0.921	0.697
2	396.9	1490.0	1280.1	9875.5	0.859	0.663
3	524.7	1490.0	1160.9	915.0	0.779	0.614
4	448.4	1490.0	1242.3	964.8	0.834	0.647
5	519.3	1490.0	1204.1	930.5	0.808	0.625
6	446.4	1490.0	1294.8	979.4	0.869	0.657
7	562.2	1490.0	1219.6	889.2	0.819	0.597
8	556.8	1490.0	1233.0	897.2	0.828	0.602
				Mean value:	0.839	0.638
				Standard deviation:	0.043	0.034
				Coefficient of variation:	5.2%	5.4%

Table 10
Comparison between test results (Yamada et al. [9]) and predicted values using ACI code and AISC-LRFD specification

Specimen no.	Eccentricity (mm)	P_{TEST} (kN)	P_{ACI} (kN)	P_{LRFD} (kN)	P_{ACI}/P_{TEST}	P_{LFRD}/P_{TEST}
1	147.5	121.0	67.6	47.6	0.559	0.393
2	82.2	217.0	135.2	80.1	0.623	0.369
3	36.2	483.0	290.5	149.0	0.601	0.309
4	78.1	200.0	128.1	74.3	0.641	0.371
5	77.0	223.0	146.3	86.3	0.656	0.387
				Mean value:	0.616	0.366
				Standard deviation:	0.038	0.034
				Coefficient of variation:	6.2%	9.2%

4.2. Observations

Based on the comparative results presented in the above section, the following observations are obtained:

1. An examination of the mean values of the predicted-to-tested capacity ratios listed in Tables 8–14 indicates that the predicted capacities based on the ACI-318 approach are about 8–25% closer to the test

Table 11
Comparison between test results (Naka et al. [10]) and predicted values using ACI code and AISC-LRFD specification

Specimen no.	Eccentricity (mm)	P_{TEST} (kN)	P_{ACI} (kN)	P_{LRFD} (kN)	P_{ACI}/P_{TEST}	P_{LRFD}/P_{TEST}
1	134.3	1470.0	1440.3	1027.0	0.980	0.699
2	239.8	980.0	934.5	682.8	0.954	0.697
3	465.8	490.0	502.2	382.5	1.025	0.781
4[a]	Infinite	214.0	203.9	191.1	0.953	0.893
				Mean value:	0.978	0.767
				Standard deviation:	0.034	0.092
				Coefficient of variation:	3.4%	12.1%

[a] Specimen no. 4 was tested under pure bending (unit: kN-m).

Table 12
Comparison between test results (Wakabayashi et al. [11]) and predicted values using ACI code and AISC-LRFD specification

Specimen no.	Eccentricity (mm)	P_{TEST} (kN)	P_{ACI} (kN)	P_{LRFD} (kN)	P_{ACI}/P_{TEST}	P_{LRFD}/P_{TEST}
1[a]	Infinite	67.7	62.9	69.2	0.930	1.022
2	246.6	293.6	312.7	266.4	1.065	0.908
3	115.2	587.1	661.4	486.6	1.127	0.829
4	67.0	880.7	925.2	670.8	1.051	0.762
				Mean value:	1.043	0.880
				Standard deviation:	0.082	0.112
				Coefficient of variation:	7.9%	12.7%

[a] Specimen No. 1 was tested under pure bending (unit: kN-m).

Table 13
Comparison between test results (Yooko et al. [12]) and predicted values using ACI code and AISC-LRFD specification

Specimen no.	Eccentricity (mm)	P_{TEST} (kN)	P_{ACI} (kN)	P_{LRFD} (kN)	P_{ACI}/P_{TEST}	P_{LRFD}/P_{TEST}
1	42.0	892.7	911.8	723.8	1.021	0.811
2	42.0	843.7	867.4	691.3	1.028	0.819
3	42.0	784.8	902.1	717.4	1.149	0.914
4	42.0	709.3	795.2	663.5	1.121	0.935
5	105.0	497.4	602.8	520.4	1.212	1.046
6	105.0	578.8	546.4	458.5	0.944	0.792
7	105.0	549.4	554.0	457.5	1.008	0.833
8	105.0	480.7	494.6	413.0	1.029	0.859
9	210.0	306.1	305.2	276.1	0.997	0.902
10	210.0	372.8	374.3	348.7	1.004	0.935
11	210.0	279.6	305.0	276.1	1.091	0.987
12	210.0	335.0	323.7	265.3	0.966	0.792
13	420.0	157.0	146.4	142.0	0.932	0.904
14	420.0	166.8	152.0	151.1	0.911	0.906
15	420.0	159.9	151.9	151.4	0.950	0.947
16	420.0	146.7	142.6	133.6	0.972	0.911
17	42.0	531.7	607.0	399.4	1.142	0.751
18	105.0	260.0	230.9	151.6	0.888	0.583
19	420.0	68.7	59.9	39.3	0.872	0.572
				Mean value:	1.013	0.853
				Standard deviation:	0.094	0.121
				Coefficient of variation:	9.3%	14.2%

results than those based on the AISC-LRFD approach. For instance, Table 9 shows that the mean value of the capacity ratio of the ACI-318 approach is 0.839 while that of the AISC-LRFD approach is 0.638. This observation reveals that the ACI-318 approach generally gives better accuracy than that of the AISC-LRFD approach in predicting the capacities of the encased composite columns.

2. Comparisons of the values of coefficient of variation (COV) listed in Tables 8–14 show that all of the COV

Table 14
Comparison between test results (Stevens [13]) and predicted values using ACI code and AISC-LRFD specification

Specimen no.	Eccentricity (mm)	P_{TEST} (kN)	P_{ACI} (kN)	P_{LRFD} (kN)	P_{ACI}/P_{TEST}	P_{LRFD}/P_{TEST}
1	19.1	716.1	672.5	523.1	0.939	0.730
2	19.1	747.3	672.5	523.1	0.900	0.700
3	19.1	898.5	672.5	523.1	0.749	0.582
4	20.3	1014.1	653.0	507.1	0.644	0.500
5	25.4	738.4	800.2	496.8	1.084	0.673
6	12.7	996.4	791.7	675.2	0.795	0.678
7	25.4	729.5	585.8	483.9	0.803	0.663
8	25.4	627.2	585.8	451.9	0.934	0.721
9	12.7	716.1	540.0	553.3	0.754	0.773
10	25.4	529.3	431.5	408.8	0.815	0.772
11	25.4	440.4	313.1	360.7	0.711	0.819
12	38.1	346.9	273.1	293.6	0.787	0.846
13	50.8	329.2	242.0	266.9	0.735	0.811
14	25.4	2989.1	2893.0	1932.7	0.968	0.647
15	50.8	2161.7	1982.5	1325.1	0.917	0.613
16	50.8	2290.7	2505.1	2057.2	1.094	0.898
17	76.2	1605.7	1610.2	1066.2	1.003	0.664
18	101.6	1316.6	1296.6	866.5	0.985	0.658
19	127.0	1165.4	1101.3	797.5	0.945	0.684
20	152.4	1027.5	929.2	641.8	0.904	0.625
21	177.8	885.2	855.8	709.0	0.967	0.801
22	203.2	747.3	749.0	602.3	1.002	0.806
				Mean value:	0.883	0.712
				Standard deviation:	0.124	0.096
				Coefficient of variation:	14%	14%

values of the ACI-318 approach are smaller than those of the AISC-LRFD approach. This observation indicates that the column capacities calculated using the ACI-318 approach are less spread than those obtained using the AISC-LRFD approach.

3. For all of the 78 column test results, Table 15 indicates that the ACI-to-experimental capacity ratio has a mean value of 0.90 with standard deviation of 0.14 and COV of 15%. On the other hand, the AISC-to-experimental capacity ratio has a mean value of 0.73 with standard deviation of 0.15 and COV of 21%.
4. Fig. 1 shows the comparison of the statistical distribution of the predicted-to-tested capacity ratio between the ACI-318 and the AISC-LRFD approaches. It is observed that the ACI-318 approach (shown as solid bars in the figure) gives a nearly bell-shaped normal distribution for the collected test results. Its peak is located at the capacity ratio between 0.9 and 1.0. On the other hand, the AISC-LRFD approach shows wider spread distribution and its peak is located at the ratio between 0.6 and 0.7. This statistical observation provides valuable infor-

Table 15
Statistical results for the 78 tested specimens listed in Tables 8–14

Reference	Numbers of tested specimen	Mean capacity ratio P_{ACI}/P_{TEST}	P_{LFRD}/P_{TEST}
Mirza et al. [7]	16	0.853	0.696
Ricles and Paboojian [8]	8	0.839	0.638
Yamada et al. [9]	5	0.616	0.366
Naka et al. [10]	4	0.978	0.767
Wakabayashi et al. [11]	4	1.043	0.880
Yokoo et al. [12]	19	1.013	0.853
Stevens [13]	22	0.883	0.712
	Mean value[a]:	0.900	0.725
	Standard deviation:	0.137	0.150
	Coefficient of variation:	15.2%	20.7%

[a] Mean value=$\sum$\{(numbers of tested specimen)×(mean capacity ratio)\}/$\sum$(numbers of tested specimen)

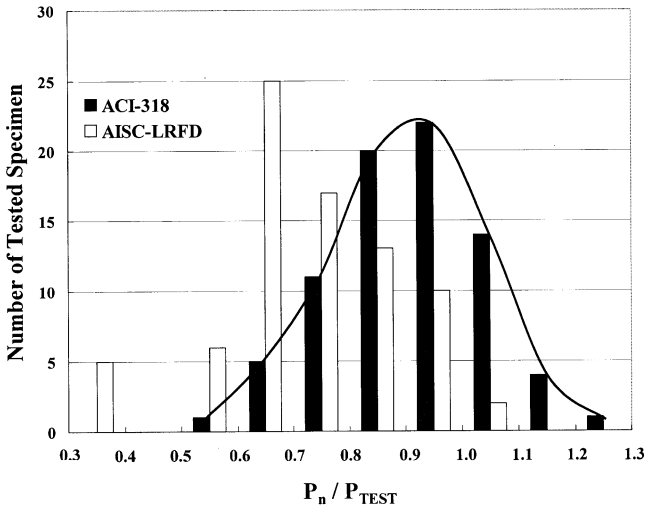

Fig. 1. Statistical distribution of predicted-to-tested capacity ratios, P_n/P_{TEST}, using ACI-318 and AISC-LRFD approaches for 78 specimens.

mation on the accuracy and reliability of the ACI-318 approach in the prediction of the strength of concrete-encased composite columns.

5. Discussions

5.1. Design philosophy

Regarding the difference of design philosophy adopted in the ACI code and the AISC specification, it is noted that the ACI-318 treats the design of concrete-encased composite columns through the extension of the design provisions for ordinary reinforced concrete columns. The ACI-318 approach considers the steel shape as an equivalent amount of reinforcement and calculates the capacity of an encased composite column based on a strain compatibility analysis procedure.

On the other hand, the AISC-LRFD approach treats the design of concrete-encased composite columns through the extension of the provisions recommended for bare steel columns. That is, the design of an encased composite column is proceeded by transforming the reinforced concrete portion into an equivalent contribution of steel shape. Then, the composite column is designed using the formulas developed for steel columns as given in Eqs. (4)–(11). It is essential to observe that these equations were originally developed for bare steel columns in which the column strength is significantly influenced by 'residual stress' and 'initial out-of-straightness' of the steel column [16,17]. However, for a concrete-encased composite column, these two parameters play a minor role because the reinforced concrete portion of the composite column is much less sensitive to the influences of residual stress and initial out-of-straightness. These observations may provide a part of the reasons why the AISC-LRFD approach gives less accurate and wider spread predictions as compared with the 78 column test results.

5.2. Failure mode

As observed from the test results [9–13], the failure modes of encased composite columns can be divided into two categories. They are: (a) bending tension failure, resulting from rebars and steel flange yielding in tension side prior to concrete crushing in compression side; (b) bending compression failure, resulting from concrete crushing and rebar buckling in compression side without yielding of rebars and steel flange in tension side.

According to the failure modes observed from the column tests, it was found that the concrete strain in extreme compression fiber was near 0.003 prior to failure [7]. This observation is consistent with the assumption made in the ACI-318 code in which the maximum concrete compressive strain is taken as 0.003.

In addition, the experimental results also revealed that the shear connectors between steel flanges and concrete had little contribution to the ultimate strength of encased composite columns [7,8]. In general, the existence of shear connectors was found to be conducive to the ACI assumption of plane section remaining plane.

5.3. Effect of steel ratio

Fig. 2 shows the distribution of the predicted-to-tested capacity ratios of the ACI and the AISC approaches corresponding to the steel ratios of the 78 tested specimens.

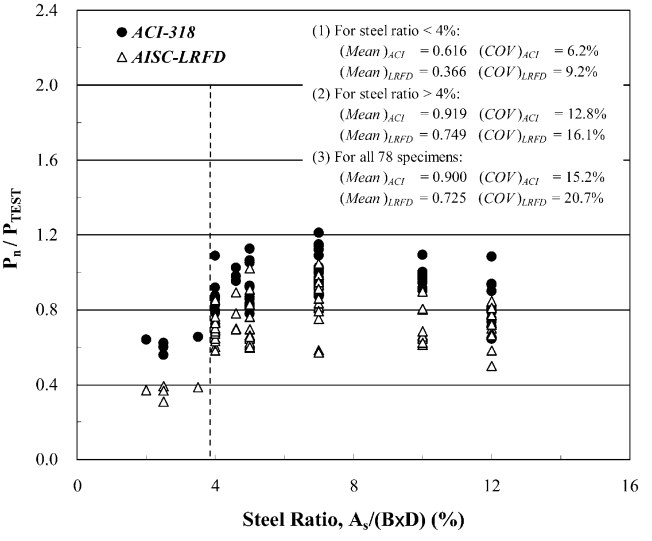

Fig. 2. Comparison of the scatter of predicted-to-tested capacity ratios, P_n/P_{TEST}, using ACI-318 and AISC-LRFD approaches for corresponding steel ratio of 78 tested specimens.

The steel ratios shown in this figure range from 2% to 12%.

For the specimens with steel ratio under 4%, it is observed that the average predicted-to-tested capacity ratios of the ACI and the AISC approaches are about 0.62 and 0.37, respectively. Both predicted-to-tested capacity ratios are found quite conservative. However, the average ratio of the ACI-318 is still about 25% closer to the test results than that of the AISC-LRFD. These observations indicated that the limitation of a minimum 4% of steel ratio in an encased composite section is essential for the AISC-LRFD strength provisions.

On the other hand, for the specimens with steel ratio near or above 4%, it is observed that the mean value of predicted-to-tested capacity ratios of the ACI-318 is 0.92, which is still more accurate than the value of 0.75 of the AISC-LRFD. In addition, the COV of the ACI-318 is found to be smaller than that of the AISC-LRFD. This means that the ACI approach also gives better predictions than the AISC approach does when steel ratio is larger than 4%.

5.4. P–M interaction diagram

As shown in Figs. 3–6, the thrust-to-moment (*P–M*) interaction diagrams of the ACI and the AISC approaches are constructed to compare with the test results. The curves with the black dots and the white spots denote the nominal *P–M* strength curves of the ACI and the AISC provisions, respectively. Eq. (12) is used to determine the nominal flexural capacity of the AISC curve.

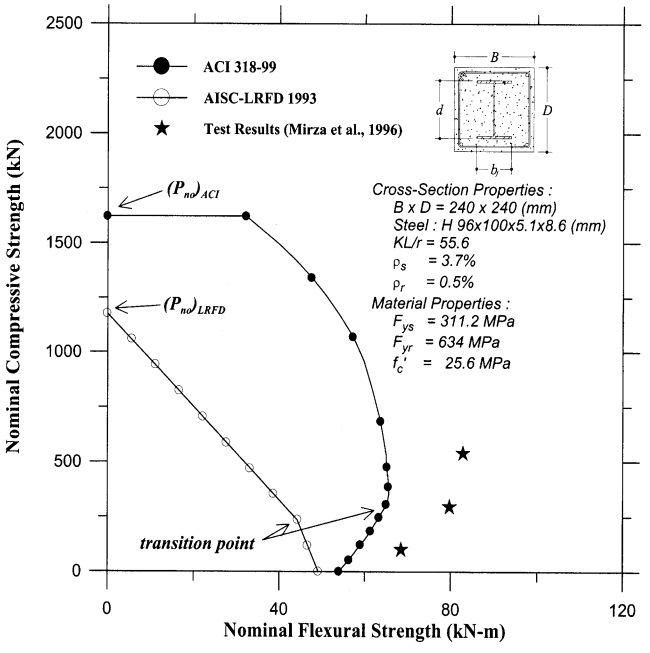

Fig. 3. Comparisons between test results [7] and nominal strengths predicted using ACI code and AISC-LRFD specification.

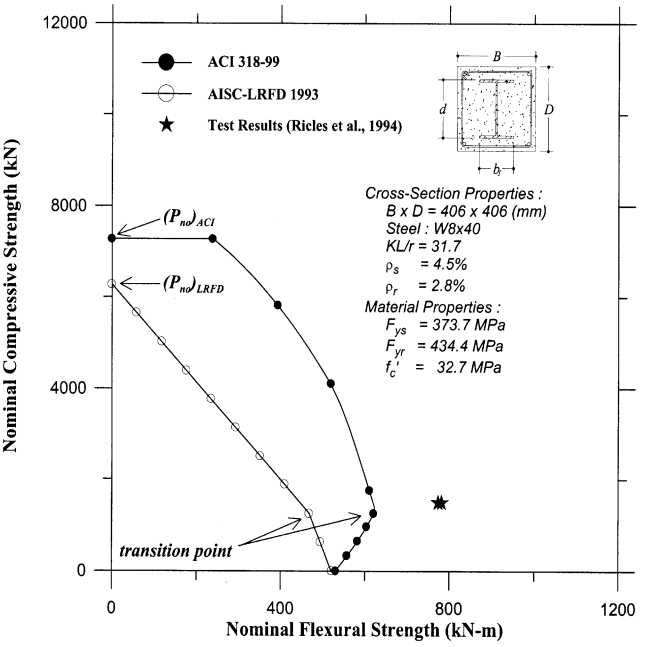

Fig. 4. Comparisons between test results [8] and nominal strengths predicted using ACI code and AISC-LRFD specification.

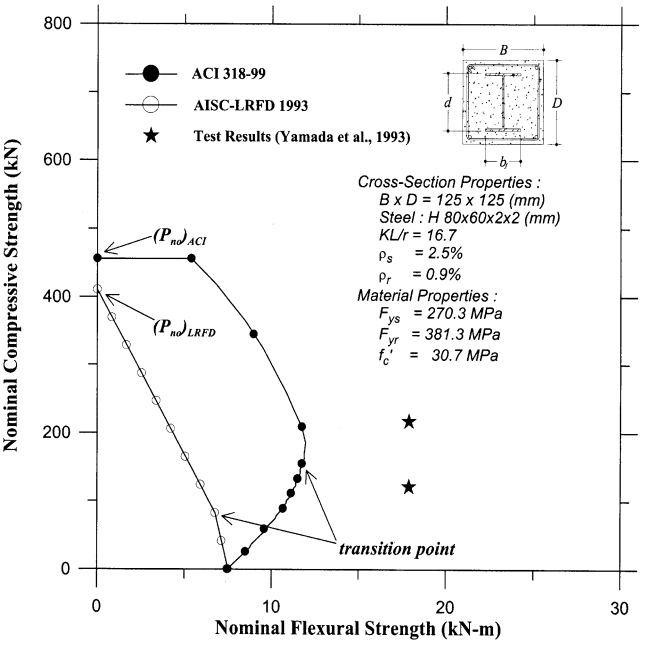

Fig. 5. Comparisons between test results [9] and nominal strengths predicted using ACI code and AISC-LRFD specification.

As compared to the column test data (denoted as stars) shown in these figures, it is observed that both the ACI and the AISC approaches give conservative estimates of the column strengths. However, the ACI curves show much closer predictions than that of the AISC curves. The comparisons indicate that the simplified bilinear *P–M* interaction equations suggested in the AISC-LRFD specification give very conservative predictions of the strength of the encased composite columns.

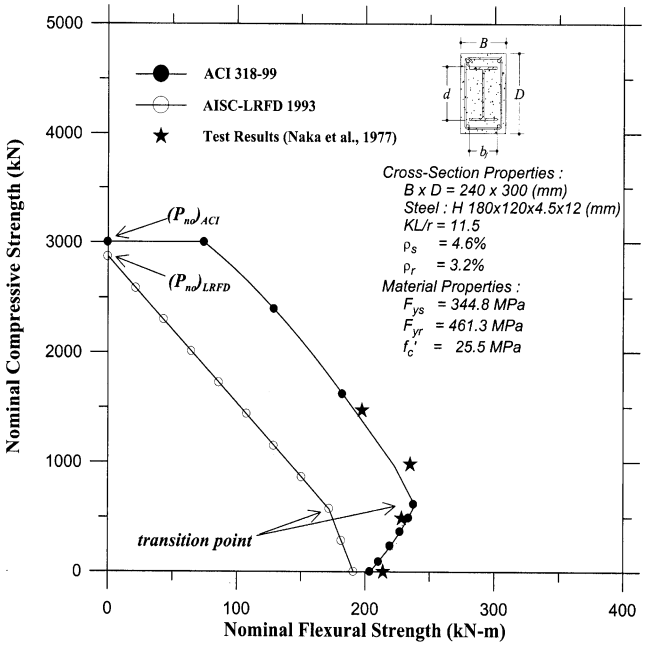

Fig. 6. Comparisons between test results [10] and nominal strengths predicted using ACI code and AISC-LRFD specification.

From these figures, it is also noted that the pure axial compressive strengths calculated by using the ACI-318 approach, $(P_{n0})_{ACI}$, are all larger than those of the AISC-LRFD approach, $(P_{n0})_{LRFD}$. The comparison between Eqs. (1a, 1b) and (4) reveals that the slenderness effect plays an important role in causing this difference. In the ACI code, the slenderness effect is accounted for only when the column slenderness ratio, KL/r, is larger than the value calculated from Eq. (3). However, in the AISC specification, all columns are subjected to the influence of slenderness effect. As shown in Eqs. (5) and (6), a slenderness parameter, λ_c, is always included in the calculation of the AISC column strength. In addition, it is found that the difference in axial strengths predicted by the ACI and the AISC approaches becomes smaller as the column slenderness ratio decreases. This is mainly because the value of the critical stress, F_{cr}, of the AISC-LRFD specification calculated from Eqs. (5) and (6) becomes larger as the value of λ_c decreases.

6. Summary and conclusions

Test results of 78 concrete-encased composite columns done by previous researchers are collected to evaluate the accuracy of the strength provisions of the ACI-318 code and the AISC-LRFD specification. The following conclusions are obtained:

1. In general, as compared with the test results, the ACI-318 approach is found to be more accurate than the AISC-LRFD approach in predicting the capacities of encased composite columns. Also observed from the comparisons is that the column capacities predicted using the ACI-318 approach are less wide spread (smaller value of coefficient of variation) than those calculated based on the AISC-LRFD approach.
2. For the 78 tested specimens, the statistical analysis on the distribution of the predicted-to-tested capacity ratios indicates that the ACI-318 approach gives a bell-shaped normal distribution curve with its peak located at the ratio between 0.9 and 1.0.
3. By observing the failure modes of the tested composite columns, the strain compatibility approach used in the ACI-318 code is found to be able to model the behavior of the concrete-encased composite columns more realistically than the section transformation approach recommended in the AISC-LRFD specification.
4. For concrete-encased composite columns with steel ratio ranging from 2 to 12%, this comparative study reveals that the ACI-318 approach shows better strength predictions than that of the AISC-LRFD. It is also observed that significant error may occur if the AISC-LRFD approach is used to calculate the capacity of an encased composite column with steel ratio under 4%.

Acknowledgements

The financial support of the National Science Council of Taiwan through contract number NSC87-2211-E009-031 is gratefully acknowledged.

References

[1] Buildings code requirements for structural concrete (ACI 318-99). Detroit (MI): American Concrete Institute (ACI), 1999.
[2] Load and resistance factor design specification for structural steel buildings. 2nd ed. Chicago (IL): American Institute of Steel Construction (AISC), 1993.
[3] NEHRP recommended provisions for seismic regulations for new buildings and other structures. Washington (DC): Building Seismic Safety Council, 1997.
[4] Viest IM, Colaco JP, Furlong RW, Griffis LG, Leon RT, Wyllie LA. Composite construction design for buildings. New York: McGraw-Hill, 1997.
[5] Furlong RW. Column rules of ACI, SSLC and LRFD compared. Journal of Structural Engineering, ASCE 1983;109:2375–86.
[6] El-Tawil S, Sanz-Picòn CF, Deierlein GG. Evaluation of ACI 318 and AISC (LRFD) strength provisions for composite beam-columns. Journal of Constructional Steel Research 1995;34:103–23.
[7] Mirza SA, Hyttinen V, Hyttinen E. Physical tests and analyses of composite steel–concrete beam-columns. Journal of Structural Engineering, ASCE 1996;122(11):1317–26.
[8] Ricles JM, Paboojian SD. Seismic performance of steel-encased composite columns. Journal of Structural Engineering, ASCE 1994;120(8):2474–94.

[9] Yamada M, Kawamura H, Zhang F. Research on the elasto-plastic deformation and fracture behaviors of wide flange steel encased reinforced concrete columns subjected to bending and shear (in Japanese). Journal of Structural Construction Engineering, AIJ (Architectural Institute of Japan) 1991;420:63–74.
[10] Naka T, Morita K, Tachibana M. Strength and hysteretic characteristics of steel-reinforced concrete columns (in Japanese). Transaction of AIJ 1977;250:47–58.
[11] Wakabayashi M, Minami K, Komura K. An experimental study on elasto-plastic characteristics of concrete members using an encased H-section subjected to combined bending and axial force (in Japanese). Bulletin of Disaster Prevention Research Institute, Kyoto University 1971;14A:417–37.
[12] Yokoo Y, Wakabayashi M, Suenaga Y. Experimental studies on steel concrete members with H-shape steel (in Japanese). Transaction of AIJ 1967;136:1–7.
[13] Stevens RF. Encased stanchions. The Structural Engineer 1965;43(2):59–66.
[14] Furlong RW. AISC column logic makes sense for composite columns, too. Engineering Journal, AISC 1976;1:1–7.
[15] SSRC, Task Group 20. A specification for the design of steel–concrete composite columns. Structural Stability Research Council (SSRC) Engineering Journal, AISC 1979;4:101–15.
[16] Bjohovde R, Tall L. Maximum column strength and multiple column curve concept. Fritz Lab. Report No. 337.29, Lehigh University, Bethlehem, PA, 1971.
[17] SSRC. Guide to stability design criteria for metal structures. 4th ed. New York: John Wiley and Sons, 1988.